# A Study on an Axial-Type 2-D Turbine Blade Shape for Reducing the Blade Profile Loss

**Soo-Yong Cho***
*Gyeongsang National University, Department of Aerospace and Mechanical Engineering, Kyungnam 660-701, Korea*
**Eui-Soo Yoon, Bum-Seog Choi**
*Korea Institute of Machinery and Materials, Department of Fluid Thermal and Environmental Engineering, Daejeon 305-343, Korea*

Losses on the turbine consist of the mechanical loss, tip clearance loss, secondary flow loss and blade profile loss etc.,. More than 60 % of total losses on the turbine is generated by the two latter loss mechanisms. These losses are directly related with the reduction of turbine efficiency. In order to provide a new design methodology for reducing losses and increasing turbine efficiency, a two-dimensional axial-type turbine blade shape is modified by the optimization process with two-dimensional compressible flow analysis codes, which are validated by the experimental results on the VKI turbine blade. A turbine blade profile is selected at the mean radius of turbine rotor using on a heavy duty gas turbine, and optimized at the operating condition. Shape parameters, which are employed to change the blade shape, are applied as design variables in the optimization process. Aerodynamic, mechanical and geometric constraints are imposed to ensure that the optimized profile meets all engineering restrict conditions. The objective function is the pitchwise area averaged total pressure at the 30 % axial chord downstream from the trailing edge. 13 design variables are chosen for blade shape modification. A 10.8 % reduction of total pressure loss on the turbine rotor is achieved by this process, which is same as a more than 1 % total-to-total efficiency increase. The computed results are compared with those using 11 design variables, and show that optimized results depend heavily on the accuracy of blade design.

**Key Words:** Turbine Blade Design, Turbine Blade Optimization, Axial-Type Turbine, Shape Parameters, 2-D Turbine Blade, Compressible Flow Analysis, Heavy Duty Gas Turbine

## Nomenclature

$A$ : Blade sectional area
$Cl$ : Blade loading coefficient (lift/dynamic pressure)
$Cp$ : Pressure coefficient
Cx : Axial chord length
Ct : Tangential chord length
$ds$ : Length between the inflection points
$h$ : Enthalpy
$k$ : Turbulence kinetic energy
$P$ : Pressure
$P_t^*$ : Total pressure normalized by double of dynamic pressure
$Re$ : Reynolds number
$T$ : Temperature
$v$ : Absolute velocity
$w$ : Relative velocity
$x$ : Axial length from the leading edge on a blade
$xl$ : Violating length by the inflection point

* Corresponding Author,
**E-mail** : sycho@nongae.gsnu.ac.kr
**TEL** : +82-55-751-6106; **FAX** : +82-55-757-5622
Gyeongsang National University, Department of Aerospace and Mechanical Engineering, Kyungnam 660-701, Korea. (Manuscript **Received** October 17, 2001; **Revised** April 15, 2002)

$X$ : Design variables
$Y$ : Total pressure loss coefficient
$\beta$ : Flow angle
$\varepsilon$ : Turbulence dissipation rate
$\theta$ : Angle on the blade surface
$\rho$ : Density
$\sigma$ : Standard deviation
$\xi$ : Enthalpy loss coefficient

**Subscripts**

0 : Initial value
in : Inlet flow condition
out : Outlet flow condition
N : Nozzle
R : Rotor
t : Stagnation
t-t : Total-to-total
$\infty$ : Value at reference location
1,2,3 : Nozzle inlet, nozzle exit, rotor exit

## 1. Introduction

Turbine efficiency is the most important factor on the performance of heavy duty gas turbines for power plants, air turbines, or turbo expanders etc.,. This efficiency is related very closely with losses in the passage. Losses on the turbine consist of mechanical losses due to the friction of rotating parts or bearings, tip clearance losses due to the flow leakage through tip gap, secondary flow losses due to curved passages, and profile losses due to the blade shape. The two latter loss mechanisms cause to generate more than 60 % of total loss on the turbine (Cofer et al., 1993). These losses could be reduced by how a turbine blade shape is designed. So, it needs to develop a new design technology for providing an optimum turbine blade profile.

The turbine blade thickness has to be thick compared with typical airfoil shapes because its blade should endure the tension stress which is caused by the centrifugal force generated on the operating conditions, such as high temperature and high RPM. Generally, blade profiles have been designed according to the inlet and exit conditions also considering the aerodynamic characteristics such as incidence or deviation angle as well as the structural characteristics. Many methods of designing blade profiles have been developed such as a method using multi-polynomial (Engeli et al., 1978), a method using shape parameters (Pritchard, 1985 ; Cho et al., 2000), and an inverse method (Demeulenare and Braembussche, 1998) etc.,. Although blades have been designed according to the design point using any one among several methods, the relationship between the blade shape and its efficiency is not known.

A 3-D turbine blade is usually designed by stacking 2-D blade profiles which are designed according to the flow conditions at several radial locations, therefore; the optimization of the 2-D blade profile affects greatly to the efficiency of the 3-D turbine blade. Recently, an optimization process was applied to design an axial compressor blade (Lee and Kim, 2000). On a turbine blade, it was tried by using Bezier curves (Goel et al., 1996; Pierret, 1999). In this study, shape parameters, which can modify the blade profile directly, are employed to optimize a 2-D blade profile. This method has several advantages over other approaches, one is that it can figure out the relationship between a blade profile and its efficiency directly because the blade profile is controlled by shape parameters.

It is selected the pitchwise area averaged total pressure at 30 % axial chord downstream from the trailing edge as an objective function. It can be maximized without losing the blade loading and blade sectional area. This is same to minimizing the total pressure loss in the passage. The results obtained with 13 design variables are compared with those using 11 design variables. This method could be applied to develop a high efficiency turbine blade as well as to modify a turbine blade for improving efficiency.

## 2. Selection of Design Variables

### 2.1 Optimum design variables

Shape parameters, which can be used to design general axial-type turbine blades, are induced from a seriously twisted turbine blade. Table 1 and Fig. 1 show these parameters, which are suf-

**Table 1** List of shape parameters for designing axial-type turbine blade profiles

| |
|---|
| Blade radius ($R$) |
| Axial and tangential chord (Cx, Ct) |
| Inlet upper wedge angle ($\varepsilon_{up}$) and lower wedge angle ($\varepsilon_{lo}$) |
| Half of major axis ($\eta_{ux}$) and minor axis ($\eta_{uy}$) of upper ellipse |
| Half of major axis ($\eta_{lx}$) and minor axis ($\eta_{ly}$) of lower ellipse |
| Inlet blade angle ($\beta_{in}$) and exit blade angle ($\beta_{out}$) |
| Unguided turning angle ($\zeta$) |
| Number of blade (N) |
| Leading and trailing edge radius ($r_{le}$, $r_{te}$) |
| Leading and trailing edge turning angle ($\kappa$, $\lambda$) |
| Turning angle on pressure surface ($\varphi$) |
| Peak point of suction surface (Sx, Sy) |
| Peak point of pressure surface (Px, Py) |
| Throat (o) |
| Straight section of trailing edge ($d_{te}$) |

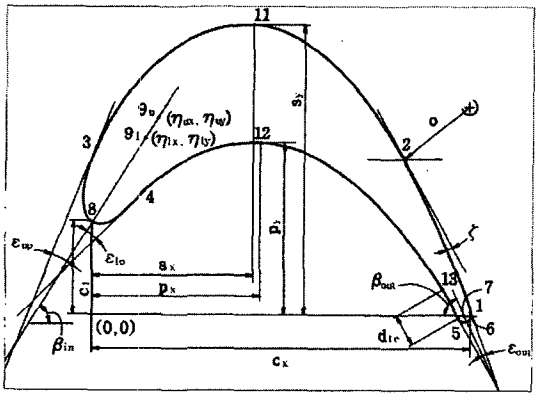


**Fig. 1** Shape parameters for designing general axial-type turbine blades

ficient enough to design general axial type turbine blades.

It is preferred to use a minimum number of shape parameters to design a blade profile because it lessens the time involved. However, the chosen minimum number of shape parameters should not make it hard to express the blade profile precisely. If many shape parameters are used, the blade profile can be expressed well and its flexibility can control the profile locally. However, it requires a lot of computational time for optimization and makes the blade design

**Table 2** Shape parameters and design variables for blade optimization

| Shape parameters | Design variables |
|---|---|
| $\zeta$ | $\theta_2$, $\theta_1$ |
| $\varepsilon_{up}$ | $\theta_3$, pt3 ($x_3$, $y_3$) |
| $\varepsilon_{lo}$ | $\theta_4$, pt4 ($x_4$, $y_4$) |
| $\varepsilon_{out}$ | $\theta_5$, $\theta_1$ |
| $\eta_{ux}$, $\eta_{uy}$ | $\theta_3$, pt3 ($x_3$, $y_3$ |
| $\eta_{lx}$, $\eta_{ly}$ | $\theta_4$, pt4 ($x_4$, $y_4$) |
| o | $\theta_2$, pt2 ($y_2$) |
| $s_x$, $s_y$ | $\theta_2$, $\theta_3$, pt11 ($x_{11}$, $y_{11}$) |
| $c_t$ | pt8 ($y_8$) |

method complex. Necessary shape parameters should be selected by considering whether each shape parameter has a strong or weak effect on the blade profile. 13 shape parameters are chosen without reducing the accuracy of blade design (Cho, et al., 2000). Table 2 shows design variables related to shape parameters. Shape functions in the optimization process are not needed because the chosen design variables can change the blade profile directly.

To make a blade profile by using 13 design variables listed in Table 2, ellipse from the leading edge(pt8) to pt3 on the suction surface, 5$^{th}$ order polynomial from pt3 to the throat(pt2), and 3$^{rd}$ order polynomial from the throat to the trailing edge(pt1) are employed. On the pressure surface, ellipse from the leading edge to pt4, 3$^{rd}$ order polynomial from pt4 to pt5, and circle at the trailing edge(pt5-pt1) are employed. In order to study the effect relating to the accuracy of blade design, the computed results using 13 shape parameters are compared with those using 11 shape parameters. In case of using 11 design variables, pt11 is not applied as the shape parameter, therefore ; 3$^{rd}$ order polynomial from pt3 to the throat and circle from the throat to the trailing edge on the suction surface are employed.

Fig. 2 shows redesigned blade profiles with 13 or 11 design variables. The mark in the figure means an original blade profile and lines mean the redesigned blade profiles. It shows some deviations between the original and redesigned blade profile using only 11 design variables at the fore part of suction surface. However, the redes-

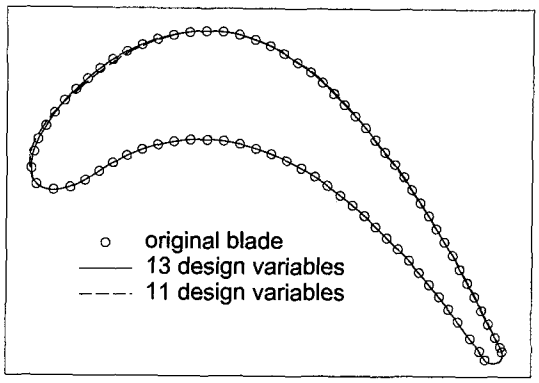


**Fig. 2** Comparison of redesigned blade profiles using 11 or 13 design variables

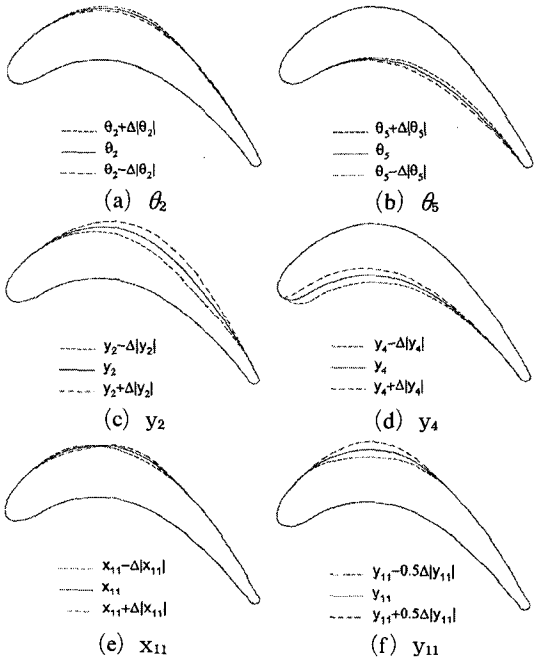


**Fig. 3** Blade profiles controlled with various design variables

igned blade profile with 13 design variables fits well with the original blade profile.

The standard deviation($\sigma$) between the original and redesigned blade profile is calculated. $\sigma$ of the blade profile designed by 11 design variables is 0.45 % on the suction surface and 0.17 % on the pressure surface, so totally it is less than 0.33 %. In case of 13 design variables, $\sigma$ on the suction surface is less than 0.17 % and totally less than 0.17 %. The accuracy of blade design is increased almost 50 % by adding two design variables i.e., $x_{11}$, $y_{11}$ which are shown in Fig. 1.

### 2.2 Controllability of design variables

Figure 3 shows how various blade shapes are controlled by design variables. For reference, only six variables among 13 design variables are selected, and 10 % of design value is used as the variance for easy identification. In the optimization, blade profile is continuously modified by new values of design variables.

## 3. Optimization and Flow Analysis Algorithm

### 3.1 Objective Function and Constraints

We can choose the blade loading as an objective function on the turbine blade, but the increment of blade loading should be accompanied with the increment of blade area due to larger torsional stress. In this study, total pressure loss instead of blade loading is chosen as an objective function. Minimizing the total pressure loss is equivalent to maximizing the pitchwise area averaged total pressure at 30 % axial chord, which is approximately axial gap between blade to blade, downstream from the trailing edge. Constant total pressure is maintained at the inlet during optimization.

$$\text{Maximize ; obj}=P_t(X) \text{ at x}=1.3Cx \qquad (1)$$
$$A \geq A_0$$
$$Cl \geq Cl_0$$

Constraints are applied to the initial blade sectional area and blade loading, and these values should not decrease lower than initial values in the optimization process. Another constraint comes from geometric conditions. Ellipse is applied to the shape of the leading edge, and its shape depends on the inlet wedge angle. To use an ellipse as a blade profile, maximum and minimum wedge angles should be restricted not to generate a wiggled profile.

5th order polynomial is applied to the suction surface. Depending on the pt11, the suction surface could be wiggled. In order to make a smooth and uniform surface, the existence of an inflection

**Table 3** Initial values of objective function and constraints

| Contents | 11 design variables | 13 design variables |
|---|---|---|
| Area ($A_5$) | 0.2133 | 0.2137 |
| Blade loading coefficient ($Cl_0$) | 1.467 | 1.469 |
| Total pressure ($P_{t0}$*) | 2.9037 | 2.9098 |

point at the interior region between pt2 and pt3 should be avoided. If one inflection point exists, the degree of deviation from the condition to make a smooth curve could be set as follows;

$$xl=-\min[ds1,\ ds2] \tag{2}$$

where $ds1$ and $ds2$ is the length between inflection point and x2 or x3, respectively. If two inflection points exist, the surface is worse than the worst curve designed when one inflection point exists. The degree of deviation could be set compared with Eq. (2) as follows;

$$xl=-[(x2-x3)/2+ds3] \tag{3}$$

where $ds3$ is the length between two inflection points. In case of three inflection points, the deviation is adjusted by considering the previous conditions as follows;

$$xl=-[(x2-x3)+ds4] \tag{4}$$

where $ds4$ is the length between the maximum and minimum inflection points. In the optimization with 13 design variables, two constraints are applied as $xl>0.05$ and $xl>0.01$ which is in fact less restrictive condition.

Table 3 shows the initial blade sectional area, blade loading coefficient and total pressure coefficient which is the pitchwise area averaged at 30 % axial chord downstream from the trailing edge and normalized by $\rho_\infty U_\infty^2$.

### 3.2 Optimization algorithm

Optimization is a procedure to find design variables($\boldsymbol{X}$), which make the objective function to be optimized (maximization, minimization, or target), without violating given constraints. The change rate of design variables is calculated as follows;

$$\Delta X^{(k)}=\alpha_k d^{(k)} \tag{5}$$

where $d^{(k)}$ and $\alpha_k$ mean new search direction and optimum move parameter of design variables in the optimization process, respectively. Optimization is deeply related to the decision of the new search direction and optimum move parameter of design variables. In this study, VisualDOC (1998), which is developed as a commercial code by Vanderplaats, is used for blade optimization. MMFD(Modified Method of Feasible Direction) among many methods is applied with constraints.

### 3.3 Flow analysis scheme

The continuity equation, momentum equations, equation of state, and energy equation are used for the compressible viscous flow analysis. These equations are derived in the vector form (Anderson et al., 1984). For turbulent flow analysis, the two-equation extended k-$\varepsilon$ turbulence model (Chen, 1989) is applied with standard wall function. Equations (6) and (7) are the turbulent kinetic energy equation and dissipation rate equation, respectively. The difference between the two-equation standard k-$\varepsilon$ turbulence model and extended k-$\varepsilon$ turbulence model occurs on the dissipation rate equation. The extended k-$\varepsilon$ turbulent model includes two time scales to allow the dissipation rate to respond to the mean strain more effectively than that of the standard k-$\varepsilon$ turbulent model (Chen and Kim, 1987). Computed results using the extended k-$\varepsilon$ turbulent model were better than those using the standard k-$\varepsilon$ turbulent model for complex turbulent flow problems (Chen, 1989; Chen and Kim, 1987).

$$\frac{\partial}{\partial t}(\rho k)+\frac{\partial}{\partial x_j}(\rho u_j k)-\frac{\partial}{\partial x_j}\left(\frac{\mu_t}{\sigma_k}\frac{\partial k}{\partial x_j}\right)=\rho(\Theta-\varepsilon) \tag{6}$$

$$\frac{\partial}{\partial t}(\rho\varepsilon)+\frac{\partial}{\partial x_j}(\rho u_j\varepsilon)-\frac{\partial}{\partial x_j}\left(\frac{\mu_t}{\sigma_\varepsilon}\frac{\partial\varepsilon}{\partial x_j}\right)=C_1\frac{\rho\varepsilon}{k}\Theta-C_2\frac{\rho\varepsilon^2}{k}+C_3\frac{\rho}{k}\Theta^2 \tag{7}$$

$$\mu_t=\rho C_\mu\frac{k^2}{\varepsilon} \tag{8}$$

where $\Theta$ is the production rate of turbulent kinetic energy. Equation (8) is the turbulence

eddy viscosity and turbulence modeling constants are as follows;

$$\sigma_k=0.75,\ \sigma_\varepsilon=1.15,\ C_1=1.15,$$
$$C_2=1.90,\ C_3=0.25,\ C_\mu=0.09$$

The governing equations are transformed to the generalized coordinates and differentiated within the finite control volume. A $2^{nd}$ order central differencing scheme is applied to the convective terms with adaptive $2^{nd}$ and $4^{th}$ order dissipation terms. The viscous and source terms of governing equations are discretized by $2^{nd}$ order central differencing scheme. A $2^{nd}$ order upwind scheme is employed for all scalar transport equations including turbulence modeling equations. A pressure based predictor/multi-corrector solution procedure is employed at the end of each time marching step. A time centered Crank-Nicholson scheme is used for the temporal discretization. To solve the system of linear algebraic equations, an iterative ADI method is employed.

In the computational region, the exit is selected at the far downstream so as not to be affected by the disturbance of passage flow, and velocities at the exit are compensated to be a constant mass flow rate. Computational blocks are inserted to avoid grid skewness and distortion at the leading and trailing edge. Inserted computational blocks improve the smoothness and orthogonality of grids. Figure 4 shows the grids developed with multi-blocks on the turbine blade.

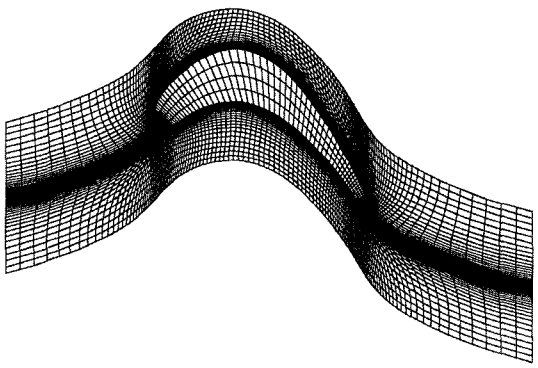

**Fig. 4** Computational grids generated with multi-blocks within a turbine passage

## 4. Results and Discussions

### 4.1 VKI turbine blade

Flow structures on the VKI turbine blade (Kiock, et al., 1986) are calculated in order to validate the flow analysis code. Flow conditions are set equally to the experimental conditions,

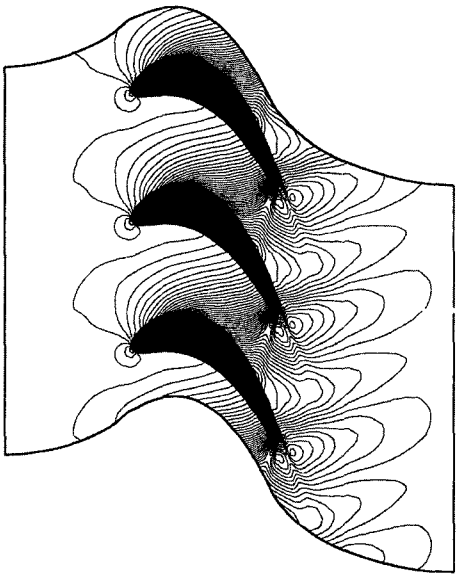

(a) Computation

(b) Experiment (Kiock et al., 1986)

**Fig. 5** Comparison of density contours within the VKI turbine passage, $Ma_{ex}=0.97$ and $Re=8.6\times10^5$

and the inlet Mach number is 0.265. As in the first case, the transonic flow is calculated. The exit Mach number is 0.96. Reynolds number and temperature at the inlet are $78.6\times10^5$ and 293K, respectively. $85\times24$ grids are employed.

Figure 5 shows the density contours compared with the experimental result (Kiock et al., 1986). Because the exit Mach number is almost 1, a shock wave occurs at the throat and an expansion wave occurs at the trailing edge. The computed results show the shock and expansion wave as shown in experimental results clearly.

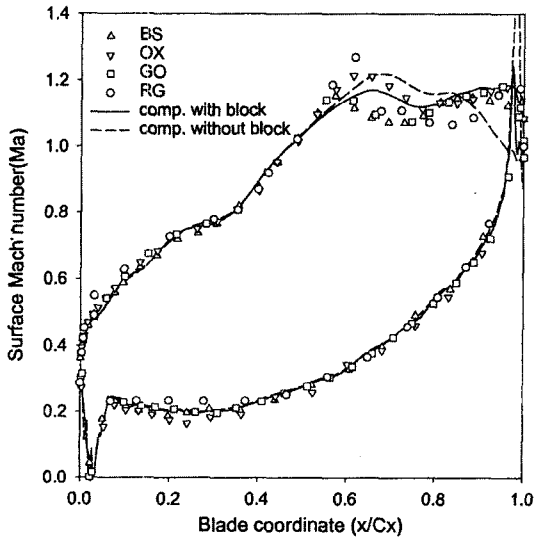


(a) Transonic flow, $Ma_{ex}=0.97$ and $Re=8.6\times10^5$

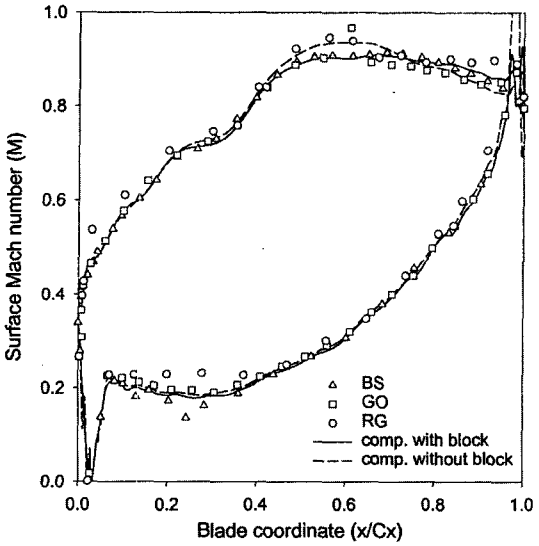


(b) Subsonic flow, $Ma_{ex}=0.78$ and $Re=7.8\times10^5$

**Fig. 6** Comparison of surface Mach numbers computed with multi-block and single block grid on the VKI turbine blade with the transonic or subsonic flow condition

Figure 6 shows the surface Mach number, which is obtained from the relationship between the surface static pressure and total pressure. In the figures, marks and lines mean the experimental data and computed results, respectively. BS, OX, GO, and RG in the figure mean that experimental results are obtained using four different facilities. The lines show the difference of computed results with or without employing multi-blocks. The computed results show that employing multi-blocks gives more stable and accurate results due to the improvement of orthogonality and smoothness of grids. Figure 6 (b) shows the surface Mach number compared with those tested in pure subsonic flow conditions. The Reynolds number and exit Mach number are $7.8\times10^5$ and 0.78, which are the same as the experimental conditions. The computed results agree well with the experimental results. As shown in Fig. 6(a), the results computed with multi-blocks are better than those with single computational block. From these results, the multi-blocks are employed in the computational region for the following turbine blade optimization.

### 4.2 Blade on a heavy duty gas turbine

A turbine rotor using on a heavy-duty gas turbine (Yoon et al., 2001) is selected and 2-D blade profile at the mean radius of turbine rotor is chosen. In the optimization process, boundary conditions at the inlet and exit are set to the operation conditions on the design point which is shown in Table 4. The inlet Mach number is 0.5462 and Reynolds number is $1.74\times10^6$. In order to decide the number of grids without grid dependence, it is calculated whether the surface pressure coefficient is converged or not according to the various grid numbers. The surface pressure coefficient is not changed even though grids are increased more than $81\times41$. $101\times51$ grids are employed for sufficient grid independence. It is necessary 3800 iterations to obtain the $0.5\times10^{-5}$

**Table 4** Operating and flow condition at the inlet and outlet to optimize a turbine blade

| Contents | Inlet | Outlet |
|---|---|---|
| Pitch (Pitch/Cx) | 0.75 | 0.75 |
| Velocity (m/sec) | $U_\infty$=393.66 | |
| Static temperature (K) | $T_\infty$=1392.01 | $T_{out}$=1366.33 |
| Static pressure (Pa) | $P_\infty$=741918 | $P_{out}$=626509 |
| Flow angle (degree) | $\beta_{in}$=61.28 | $\beta_{out}$=61.84 |
| Density (kg/m$^3$) | $\rho_\infty$=1. 86 | |

**Table 5** Values of objective function and constraints after optimization

| Contents | 11 design variables | 13 design variables with $xl$>0.05 | 13 design variables with $xl$>0.01 |
|---|---|---|---|
| Area ($A$) | 0.2133 | 0.2157 | 0.2187 |
| Blade loading coefficient ($Cl$) | 1.467 | 1.469 | 1.469 |
| Total pressure ($P_t$*) | 2.914 | 2.926 | 2.928 |

residual which is selected as the convergence condition. In this condition, the variation of objective function is less than $0.1\times10^{-3}$.

Axial chord of turbine blade is fixed in the optimization process. If the axial chord is not fixed, the objective function is meaningless, but the tangential chord length (Ct) is allowed to be changed as shown in Fig. 1. It needs 16 iterations to reach the minimum total pressure loss in the passage without violating the given constraints with 13 design variables and $xl$>0.01 constraint. Blade sectional area is increased to 2.3 % compared with the initial blade area, but the blade loading has no gain. The total pressure loss as the objective function is decreased to 10.8 %. Values of objective function, blade sectional area and blade loading coefficient are shown in table 5.

Figure 7 shows the profile difference between the original blade and optimized blade. The difference in the rear part of blade is negligible, but the fore part moves downward circumferentially. From the optimization, the tangential chord length at the leading edge is decreased and the size of fore part on the blade is reduced a little.

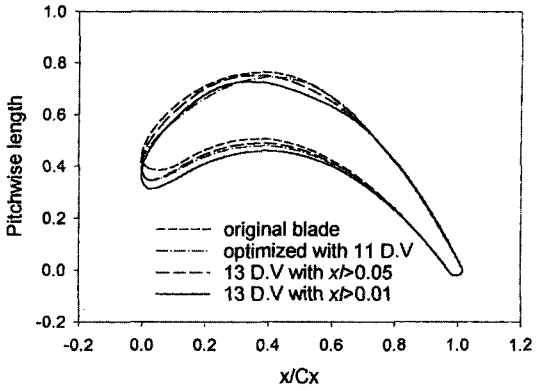


**Fig. 7** Comparison of original blade profile with optimized blade profiles

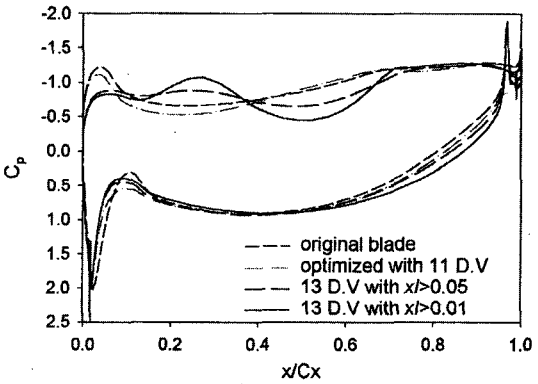


(a) Surface pressure coefficient

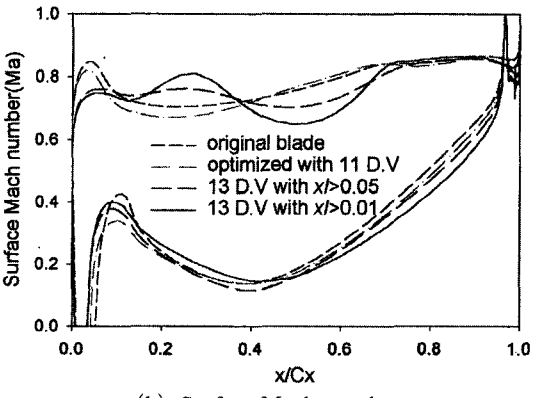


(b) Surface Mach number

**Fig. 8** Surface pressure coefficient and surface Mach number on the original and optimized blade

The reduced size of the fore part on the blade prevents a strong static pressure drop generated by fast turning flow around the leading edge, and makes the static pressure drop smoothly along the

passage. In this study, the design variables $y_{leg}$, $\theta_3$, $\theta_4$ and $y_{11}$ show strong effect to configure the optimized blade profile.

Figure 8(a) shows the surface pressure coefficient, and the phenomena mentioned in the previous paragraph are shown clearly. The small static pressure drop on the fore part of the blade makes the change of surface Mach number weak. Figure 8(b) shows that the surface Mach number is changed with the same trend as the surface pressure coefficient shown in Fig. 8(a). That is consistent because the surface pressure and Mach number are related directly with the flow area change along the passage.

Area of turbine passage is calculated by the size of circle between the pressure and suction surface. Figure 9 shows the radius of circle on blade passage optimized with 11 and 13 design variables. This figure shows that the area within the passage is expanded to the maximum area, and then reduced smoothly to the throat after passing to the peak point of suction surface. In case of employing 11 design variables, the area on the rear part of the blade is not changed. However, the changing rate of area on the optimized blade is small. This causes the reduction of total pressure loss. Figure 9(b) shows that the location of maximum area moves backward compared with the original blade. The changing rate of area on the rear part is same to the original one in case of $xl>0.01$, but is decreased in case of $xl>0.05$. However, the changing rate of area on the front part of the optimized blade is much more reduced than that of the original one. That makes the changing rate of area on the optimized blade small over the whole region as shown in Fig. 9 (a).

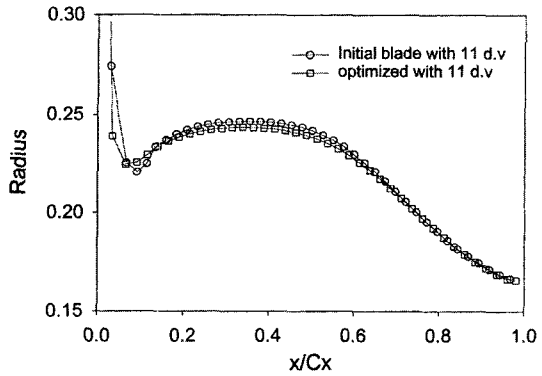


(a) With 11 design variables

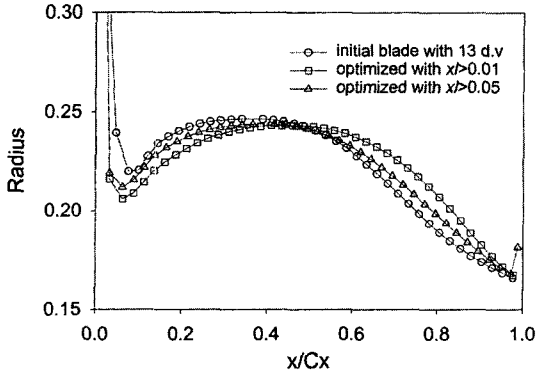


(b) With 13 design variables

**Fig. 9** Radius of circles between the pressure and suction surface within a passage to compare with the blade passage area

The reduction of total pressure loss at the exit is directly related with the efficiency increase. However, the efficiency is calculated from the enthalpy change. It needs to use the relationship between the enthalpy loss coefficient and total pressure loss coefficient. When the flow condition is in the subsonic, the total pressure loss coefficient could be simplified to $Y_N \cong \xi_N$ because the loss by shock wave is not generated within the passage. This relationship also simply applies to the rotor. The total-to-total efficiency is calculated by using the enthalpy loss coefficient from Eq. (9) defined by Horlock (1973) as follows;

$$\eta_{t-t}=\frac{1}{1+(\xi_R w_3^2+\xi_N v_2^2)\left(1+\frac{\gamma-1}{2}Ma_3^2\right)/2(h_{t1}-ht_3)} \quad (9)$$

$P_t^*$ is defined as $P_t/(\rho_\infty U_\infty^2)$, and it is related with $Y_N$ as follows;

$$Y_N=\frac{P_{t1}-P_{t2}}{\frac{1}{2}\rho_\infty U_\infty^2}=2(P_{t1}^*-P_{t2}^*) \quad (10)$$

In the computation, $Y_N$ is simplified to $\xi_N$ because the Mach number is less than 1. Before optimization, $\xi_N$ is 0.334, but $\xi_N$ is changed to 0.298 after optimization with 13 design variables having $xl>0.01$ constraints. That is 10.8 % reduction of total pressure loss. In case of $xl>0.05$,

9.8 % reduction is obtained, but 6 % reduction is obtained with 11 design variables. In order to apply these values to the Eq. (9), the denominator is assumed to be O(1.1) by considering the total-to-total efficiency on typical axial turbines. Generally, the total-to-total efficiency is calculated by the ratio of the enthalpy change obtained on the turbine in the expansion process to the enthalpy generated in the ideal process. This relation of total-to-total efficiency is modified to Eq. (9). From this relationship, a 10.8 % reduction of total pressure loss is calculated to 1 % total-to-total efficiency increase. This is obtained on only one stage of the turbine. That effect will be increased with the number of turbine stages.

Figure 10 shows the curvature of blade surface. The quick change of blade curvature causes the flow separation and pressure loss (Korakianitis, 1993). It is important to design a smooth blade profile. Constant curvature is generated on the rear part of suction surface because the circle is applied to that area. The changing rate of curvature on the optimized blade with 11 design variables is smooth. Figure 10(b) shows the curvature of blade surface optimized with 13 design variables. On the suction surface, the sign of curvature is not changed because the inflection point is avoided. Even the changing rate of curvature on the optimized blade is increased compared with the original one, it is not as steep but changes smoothly over the whole region. In case of $xl>0.01$, the changing rate of curvature is increased compared with that of $xl>0.05$ because it is more alleviated constraint.

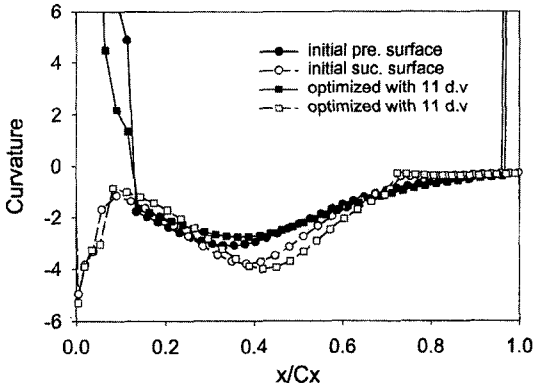


(a) With 11 design variables

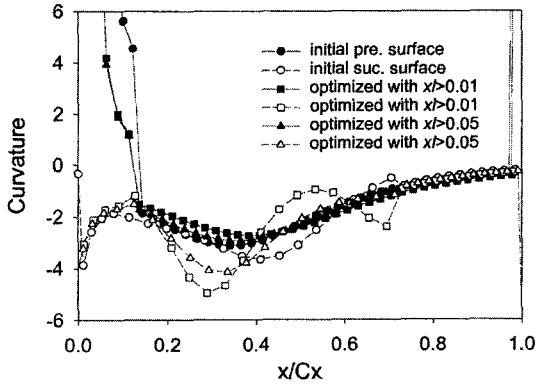


(b) With 13 design variables

**Fig. 10** Curvatures on the pressure and suction surface of blades

## 5. Conclusions

The blade is designed using shape parameters, and optimized. The axial chord of blade is fixed, and 11 or 13 design variables are employed for optimization. The pitchwise area averaged total pressure at the 30% axial chord downstream from trailing edge, which is the inlet location of next turbine blade, is selected as an objective function. Without reducing initial blade sectional area and blade loading, 10.8% of total pressure loss in the passage is reduced by employing 13 design variables. This is the same as a 1% increase of total-to-total efficiency on the one stage of turbine. The efficiency will be increased with the number of turbine stage.

Optimizing the turbine blade, the changing rate of blade passage area on the optimized blade is reduced compared with that of the original one. This causes the reduction of profile loss and total pressure loss. On the blade profile, the radius of leading edge and the circumferential length at the leading edge are decreased on the optimized blade. However, the blade shape at the rear part of blade i.e., from the throat to the trailing edge, keeps the original profile.

The value of objective function depends on the accuracy of blade design. The accuracy of blade design with 13 design variables is increased 50 % more than that with 11 design variables. By this,

the value of objective function is increased 80 % more. In the optimization, the accuracy of blade design is an important factor and affects the result of objective function.

In the actual application, the optimization of 3-D blade is necessary. The method using shape parameters should be expanded to the 3-D blade.

## Acknowledgment

The Authors would like to thank the ReCAPT (Research Center of Aircraft Parts Technology) and BK21 for funding this project.

## References

Anderson, D. A., Tannehill, J. C. and Pletcher R. H., 1984, *Computational Fluid Mechanics and Heat Transfer*, McGraw-Hill, pp. 181~197.

Chen, Y. S., 1989, "Compressible and Incompressible Flow Computations with a Pressure Based Method," *AIAA-89-0286*, 27th Aerospace Science Meeting.

Chen, Y. S. and Kim, S. W., 1987, "Computation of Turbulence Flows using a Extended k-$\varepsilon$ Turbulence Closure Model," *NASA CR*-179204.

Cho, S. Y., Oh, K. S. and Choi, B. S., 2000, "A Study of Design Parameters for Designing an Axial Turbine Blade Geometry," In *Proceedings of the 8th International Symposium on Transport Phenomena and Dynamics of Rotating Machinery*, Hawaii, Vol. 1, pp. 222~228.

Cho, S. Y., Oh, K. S., Yoon, E. S. and Choi, B. S., 2000, "Study on the Minimization of Shape Parameters for Reverse Designing Axial Turbine Blade Geometry," In *The International Symposium on Energy, Environment, and Cold Region*. Kitami, No. 109.

Cofer, J. I., Reinher, J. K. and Summer, W. J., 1993, "Advances in Steam Path Technology," *GER*-3713D, pp. 1~25.

Demeulenare, A. and Braembussche, R., 1998, "Three-Dimensional Inverse Method for Turbomachinery Blading Design," *J. of Turbomachinery*, Vol. 120, pp. 247~254.

Engeli, M., Zollinger, H. J. and Allemann, J. C., 1978, "A Computer program for the design of Turbomachinery Blades," *ASME* 78-GT-36.

Goel, S., Cofer IV, J. I. and Singh, H., 1996, "Turbine Airfoil Design Optimization," *ASME* 96-GT-158.

Horlock, J. H., 1973, "Axial Flow Turbine, Robert Krieger Publishing Co.," pp. 60~66.

Kiock, R., Lehthaus, F., Baines, N. C. and Sieverding, C. H., 1986, "The Transonic Flow Through a Plane Turbine Cascade as Measured in Four European Wind Tunnels," *J. of Eng. for Gas Turbines and Power*, Vol. 108, pp. 277~284.

Korakianitis, T., 1993, "Hierarchical Development of Three Direct-Design Methods for Two-Dimensional Axial-Turbomachinery. Cascades," *J. of Turbomachinery*, Vol. 115, pp. 314~324.

Lee, S. Y. and Kim, K. Y., 2000, "Design Optimization of Axial Flow Compressor Blades with Three-Dimensional Navier-Stokes Solver," *KSME Int. J.*, Vol. 14, No. 9, pp. 1005~1012.

Pierret, S., 1999, "Three-Dimensional Blade Design by Means of an Artificial Neural Network and Navier-Stokes Solver," In *Turbomachinery Design Blade Design Systems*. Von Karman Institute Lecture Series 1999-02.

Pritchard, L. J., 1985, "An Eleven Parameter Axial Turbine Airfoil Geometry Model," *ASME* GT-85-219.

VisualDOC, 1998, "VisualDOC Reference Manual Version 1.0," *Vanderplaats R&D Inc.*

Yoon, E. S., Choi, B. S., Park, M. Y. and Park, B. K., 2001, "Development of Design and Manufacturing Technology for Cooled Turbine Blades," KIMM Report, UNC331-883M, pp. 14~57.